# Bandgap shifting of an ultra-thin InGaAs/InP quantum well infrared photodetector

D.K. Sengupta, S.D. Gunapala, S.V. Bandara, J.K. Liu, E. Luong, W. Hong, J. Mumolo, and Y. Bae

Jet Propulsion Laboratory, California Institute of Technology, Pasadena, CA 91109

G.E. Stillman, S.L. Jackson, M. Feng, S.G. Bishop, I. Adesida, S.L. Chuang, K.C. Hseih, S. Kim, A. Ping, A.P. Curtis, and H.C. Kuo

Department of Electrical and Computer Engineering, University of Illinois at Urbana-Champaign, Urbana, IL 61801

Y.C. Chang

Department of Physics, University of Illinois at Urbana-Champaign, Urbana, IL 61801

H.C. Liu

Institute for Microstructural Sciences, National Research Council, Ottawa, Canada K1A 0R6

We demonstrate that $SiO_2$ cap annealing in the ultra-thin p-type InGaAs/InP quanum wells can be used to produce large blue shifts of the band edge. A substantial bandgap blue shift, as much as 292.5 meV at 900°C have been measured and the value of the bandgap shift can be controlled by the anneal time. Theoretical modeling of the intermixing effect on the energy levels is performed based on the effective bond-orbital method and obtain a very good fit to the photoluminescence data. Compared to the as-grown detector, the peak spectral response of the annealed detector was shifted to longer wavelength without any major degradation in the responsivity characteristics.

**PACS numbers: 85.60.Gz, 42.79.Pw, 85.30.De, 73.20.Dx**

Since the first proposal of the semiconductor multiple quantum wells (MQWs) by Esaki and Tsu [1], there have been extensive theoretical and experimental studies on this subject. Detailed information about the electronic, optical, and transport properties of semiconductor MQWs has been accumulated via various experimental techniques. Theoretically, many sophisticated methods have been used to calculate the electronic band structures and optical properties of the systems. With ample knowledge about the fundamental physical phenomena available to us, we have reached the stage where combination of experimental characterization with detailed theoretical analysis can now provide meaningful engineering designs of quantum well devices that will find immediate applications. Quantum-well infrared photodetectors (QWIPs), based on intersubband absorption in III-V MQW structures, have advanced considerably in the last several years for infrared detection in the spectral regions 3-5μm and 8-12μm [2,3]. One of the distinct advantages of the quantum well approach is the ability to produce multi-band or multi-color detectors, which are desirable for future high-performance IR systems [4, 9]. Interdiffusion offers the flexibility to modify the properties of the materials after growth[10]. It is possible to modify the energy levels of QWIP after growth by rapid thermal annealing for realizing multi-wavelength response. The post growth wavelength shifting of QWIPs by rapid thermal annealing is accomplished by dielectric encapsulating the QWIP and exposing it to a high temperature for a short period of time. The quantum well is changed from a square well, with sharp interfaces, to an error-function shaped well, with a corresponding change in the confined energy levels. In addition, rapid thermal annealing can be used to broaden the spectral responses. In this letter, we present optical and device studies of the effect of intermixing on an ultra-thin (~10Å) p-type InGaAs/InP multiple quantum well structures using $SiO_2$ capping. Finally, theoretical calculations based on the effective bond-orbital method is performed to compare with the experimental results.

The detector structures were grown on an InP substrate by GSMBE using elemental In and Ga as the group III sources, while $ASH_3$ and $PH_3$, injected through separate fast-switching low pressure crackers, were used as the group V sources. Elemental Be was used as its p-type dopant. The substrate temperature was kept constant at 500°C during the growth of the various layers. In

order to improve interface quality, an optimized switching scheme was developed and used for its transition from InP to InGaAs as well as the transition from InGaAs to InP[11]. The p-type structure consisted of 30 periods of 10Å center doped ($p = 3x10^{18}cm^{-3}$) $In_{0.53}$ $Ga_{0.47}$ As quantum wells and 500Å thick, uniformly Be doped ($p = 1x10^{17}cm^{-3}$) InP barriers, all of which were sandwiched between 5000Å Be doped ($p = 3x10^{18}cm^{-3}$) $In_{0.53}$ $Ga_{0.47}$ As contacts on an InP substrate.

In all studies, prior to annealing the samples were first degreased in trichlorethane, acetone, and methanol followed by a light surface etch using $NH_4OH$. Then, a 1500Å $SiO_2$ encapsulant was deposited by plasma enhanced chemical vapor deposition. Rapid thermal annealing was performed in an AET RTA reactor with 10 sccm of $N_2$ flowing. The temperature was stabilized at 200°C prior to the high temperature annealing.

The optical properties of the as-grown and annealed QWIP samples were investigated using low temperature photoluminescence measurements. In the PL measurements, the MQW sample was mounted in a He cryostat and excited by the 632.8 nm line of He-Ne laser. A low excitation density (<1 $W/cm^2$) was used to obtain excitonic recombinations. The emission spectrum was dispersed in a 0.5m SPEX monochromator and detected with a $LN_2$ cooled Ge detector.

In Figure 1(a), the 6K PL spectrum of as-grown and annealed InGaAs/InP QWIP samples are shown. A blue shift (~24.0 meV @ 700°C, ~130.2 meV @ 800°C and ~292.5 meV @ 900°C) of photoluminescence peak was observed. This is expected, as the grown state is higher and the effective barrier height lower for the annealed QWIP than the as-grown QWIP. In addition to the blue shift, the annealed QWIP samples also exhibit a reduction in the peak luminescent intensity and is attributed to the out-diffusion of the p-type (Be) dopants from the well and is strongly dependent on the amount of disordering during the annealing process. Rapid thermal annealing at 900°C leads to a blue shift of ~292.5 meV and almost complete alloying. In Figure 1 (b), 6K PL spectrum of the as-grown and annealed (800C ) InGaAs/InP QWIP samples at 20, 40, and 60 sec are shown. A blue shift (~ 108 meV for 20 sec, ~ 135 meV for 40 sec and ~ 150 meV for 60 sec) of the photoluminescence peak was observed. Figure 2 shows the PL half width of the emission line versus the annealing temperatures. Up to an annealing temperature of 800°C, the half width of

the luminescence spectrum remain approximately 19.3 to 19.6 meV and results in no significant degradation of the PL linewidth up to 800°C rapid thermal annealing.

In summary, we have achieved strong and homogeneous intermixing in InGaAs/InP MQWs, using $SiO_2$ capping and subsequently annealing. No significant degradation of optical properties was observed up to 800°C. A substantial PL blue shift, as much as 130.2 meV, was found in the structure and the value of the shift can be controlled by its anneal time. In addition, beyond 800°C annealed QWIP structure also exhibits a reduction in peak luminescent intensity, which may be due to the overall broadening of the peak response as well as any defects the annealing process might have introduced.

Quantum well infrared photodetectors were fabricated from the as-grown and $SiO_2$ encapsulated annealed samples into 200μm circular mesas by etching through the upper contact layer and the multiple quantum well structure down to the bottom contact layer. Ohmic contacts to the p-doped contact layers were subsequently formed by evaporating and alloying Ti/Pt/Au metallization. Spectral response and absolute responsivity measurements on the as-grown and annealed QWIPs were performed with its detectors mounted on a stage which is in thermal contact with the cold end of a continuous flow helium cryostat. The detectors were connected to an external bias circuit, and bias supplied using a battery in series with a large resistor. The absolute magnitude of the responsivity was determined by measuring the blackbody response with a calibrated blackbody source of 1000K. Figures 3(a) & (b) show the photoresponses for both the as-grown and annealed detector with bias. The peak response wavelength measured were ~4.55μm (80K, 5.9V) for the as-grown detector and ~7.0μm (4.5K, 4V) for the annealed detector. Since the ground state is higher and the effective barrier height is lower in the annealed detector than in the as-grown detector, the peak response wavelength of the annealed detector experiences a long wavelength shift. The peak absolute responses were calculated to be ~2.5 mA/W (80K and 5.9V) for the as-grown detector and ~2.0 mA/W (4.5K and 4V) for the annealed detector from the blackbody and relative spectral responses. The peak absolute responsivity of the annealed detector is of a similar magnitude compared to the as-grown detector and the small

reduction in the broadened response is attributed to the out-diffusion of the Be-dopant from the well.

Theoretical modeling of the intermixing effect on the energy levels is performed based on the effective bond-orbital method (EBOM). This method casts the k.p formalism into a local-orbital formalism so that the complicated boundary conditions in heterostructures can be easily managed. Details of this method is given in Ref.[12]. This method has been used to calculate the electronic structures and optical response of many kinds of multiple quantum wells (MQW's), including GaAs-$A1_xGa_{1-x}As$[12], InAs-GaSb[12], HgTe-CdTe[13], and GaInAs-InP[14] with good success. Here we are interested in the intermixing effect in $In_{0.53}Ga_{0.47}As$/InP MQW's. Both Group III (Ga) and Group V (P) interdiffusion will be considered. Prior to the interdiffusion, the system is strain-free. After the interdiffusion, there is a weak strain distribution, whose effect on the electronic states is modeled according to the Bir-Picus theory [15]. Furthermore, with the interdiffusion, the system turns into a InGaAsP quaternary compound with compositional modulation. The input band parameters used in our modeling are listed in Table I. Here $E_v$ and $E_c$ are the zone-center energies for the valence band and conduction band, respectively. Note that we use the experimental band gap of bulk $In_{0.53}Ga_{0.47}As$ as the input parameter rather than the linear interpolation of band gaps of InAs and GaAs, since the band-gap bowing effect is significant for InGaAs alloy.

The model system for the as-grown sample is a superlattice with each period consisting of 4 monolayers (11A) of $In_{0.53}Ga_{0.47}As$, one monolayer of $InAs_{0.5}P_{0.5}$ and 169 monolayers (497A) of InP. The presence of one monolayer of $InAs_{0.5}P_{0.5}$ is suggested by the DCXRD analysis. Including this $InAs_{0.5}P_{0.5}$ monolayer at one interface between $In_{0.53}Ga_{0.47}As$ and InP in our model also makes the resulting energy gap (1.102 eV) in better agreement with the PL measurement (1.082 eV). Without this $InAs_{0.5}P_{0.5}$ monolayer, the energy gap obtained in our model would have been 0.05 eV higher. The difference of 20 meV between the theoretical bandgap predicted here and the PL peak position can be attributed to the excitonic effect (which accounts for approximately 10 meV) and the effects due to difference in the realistic geometry and the ideal geometry used

here. With intermixing, the difference in the realistic geometry and the ideal geometry used here. With intermixing, the systems turns into a $In_{1-x}Ga_xAs_{1-y}P_y$ quaternary superlattice with both x and y being functions of z (the coordinate in growth direction). Since x is close to 0.47 in the well region and 0 in the barrier region, we obtain the EBOM parameters for $In_{1-x}Ga_xAs_{1-y}P_y$ by taking the linear interpolation between the corresponding EBOM parameters for $In_{0.53}Ga_{0.47}As_{1-y}P_y$ $InAs_{1-y}P_y$ and via the following relation

$$V(In_{1-x}Ga_xAs_{1-y}P_y) = (x/0.47)V(In_{0.53}Ga_{0.47}As_{1-y}P_y) + (1-x/0.47)V(InAs_{1-y}P_y),$$

where $V(In_{0.53}Ga_{0.47}As_{1-y}P_y) = (1-y)V(In_{0.53}Ga_{0.47}As)+yV(In_{0.53}Ga_{0.47}P)$

and $V(InAs_{1-y}P_y) = (1-y)V(InAs)+yV(InP)$.

The composition (x or y) distribution is modeled by a simple diffusion theory[16]. For Group III (Ga) interdiffusion, we obtain

$$x = 0.47\ \{erf[(L/2+z)/2\sqrt{D_1t}] + erf[(L/2-z)/2\sqrt{D_1t}]\}/2$$

and for Group V (P) interdiffusion, we have

$$y = 1 - \{erf[(L/2+z)/2\sqrt{D_2t}] + erf[(L/2-z)/2\sqrt{D_2t}]\}/2$$
$$- \{erf[(a_1/2+z_1)/2\sqrt{D_2t}] + erf[(a_1/2-z_1)/2\sqrt{D_2t}]\}/2,$$

where $D_1$ and $D_2$ are the diffusion constants for describing Ga and P interdiffusions, respectively and t is the annealing time. L is the width of the quantum well and z is distance measured from the center of the well. The second term in the expression for y(z) describes the interdiffusion due to the one monolayer $InAs_{0.5}P_{0.5}$ monolayer. The diffusion constant is determined by fitting the calculated band gap energies to the experimental results. With $D_1$ =7.03 x $10^{-17}$ $cm^2/s$ and $D_2$ = 3.92 x $10^{-17}$ $cm^2/s$ we obtain a very good fit to the PL data as shown in Figure 4(b). In Figure 4(a)&(b), the dotted line shows the calculated band gap as a function of the annealing time with Group V (P) interdiffusion alone and the dashed line shows the results with both Group III and Group V interdiffusions. To compare with the PL data, we have rigidly shifted the calculated band gap by 20 meV downward so that the calculated results for as-grown sample agree with the PL data. We found that the Group III (Ga) interdiffusion has much smaller effect on the band gap shift compared with the Group V (P) interdiffusion. This also means that the

diffusion constant for Group III interdiffusion obtained by fitting the PL data is subject to a much larger error.

In conclusion, we have demonstrated that rapid thermal annealing can be employed to both shift the operating wavelengths and to broaden the response of an ultra-thin p-type InGaAs/InP quantum well infrared photodetector following intermixing of the well and barrier layers during rapid thermal annealing. The intermixing effect on the energy levels is performed based on the effective-bond orbital method and obtain a very good fit to the PL data. The use of rapid thermal annealing changes the well profile of a QWIP and peak wavelength making feasible integration of multiple colored pixels.

Research described in this paper was performed by the Center for Space Microelectronics Technology, Jet Propulsion laboratory, California Institute of Technology, Pasadena, CA 91109 and was sponsored by the NASA Office of Space Science and by the Microelectronics Laboratory, University of Illinois at Urbana-Champaign, Urbana, IL 61801. The authors would like to thank Prof. N. Holoynak of University of Illinois at Urbana-Champaign and Prof. E.H. Li of the University of Hong Kong and the members of the Semiconductor Research Group, University of Illinois at Urbana-Champaign for many helpful discussions. We would also like to acknowledge D. Cuda (JPL) for the help with the manuscript preparation. One author (D.K.S.) acknowledges the fellowship awarded by the National Academy of Sciences – National Research Council.

## References


[1] L. Esaki and R. Tsu, IBM J. Res. Develop. 14, 61 (1970).

[2] B.F. Levine, J. Appl. Phys. 74, R1-R81 (1993).

[3] S.D. Gunapala, S.V. Bandara, J.K. Liu, W. Hong, M. Sundaram, R. Carralejo, C.A. Shott, P.D. Maker, and R.E. Muller, SPIE proceedings, V 3061, 124 (1997)

[4] S.D. Gunapala and S.V. Bandara, Physics of Thin Films, edited by M.H. Francombe, and J.L. Vossen, Vol. 21, pp. 113-237, Academic Press, NY, (1995).

[5] I. Grave, A. Shakouri, N. Kuze, and A. Yariv, Appl. Phys. Lett. 60, 2362 (1992).

[6] A. Kock, E. Gornick, G. Abstreiter, G. Bohn, M. Walther, and G. Weimann, Appl. Phys. Lett. 60, 2011 (1992).

[7] Y.H. Wang, Sheng S. Li, and P.Ho, Appl. Phys. Lett. 62, 93 (1993).

[8] E. Martinet, E. Rosencher, F. Luc, Ph. Bois, E. Costard, and S. Delaitre, Appl. Phys. Lett. 61, 246 (1992).

[9] K. Kheng, M. Ramsteiner, H. Schneider, J.D. Ralston, F. Fuchs, and P. Koidl, Appl. Phys. Lett. 61, 666 (1992).

[10] D.G. Deppe, L.J. Guido, N. Holonyak Jr., K.C. Hseih, R.D. Burnham, R.L. Thornton and T.L. Paoli, Appl. Phys. Lett. 59, 510 (1986).

[11] S.L. Jackson, J.N. Baillargeon, A.P. Curtis, X. Liu, J.E. Baker, J.I. Malin, K.C. Hseih, S.G. Bishop, K.Y. Cheng, and G.E. Stillman, J. Vac. Sci. Technol. B 11, 1045 (1993).

[12] Y.C. Chang, Phys. Rev B 37, 8215 (1988).

[13] Y.C. Chang, J. Cheung, A. Chiou, and M. Khosnevisan, J. Appl. Phys. 66, 829 (1989).

[14] M.P. Houng and Y.C. Chang, J. Appl. Phys. 65, 3092 (1989).

[15] G.L. Bir and G.E. Pikus, Symmetry and Strain Induced Effects in Semiconductors (Halsted, United Kingdom, 1974).

[16] Choy, J. Appl. Phys. 82, 3861 (1997).

## Figure captions

Fig. 1(a) Photoluminescence spectra at 6K of the as-grown and RTA (700C, 800C, and 900C for 30s) MQW structures.

Fig. 1(b) 6K photoluminescence spectra of the as-grown and RTA treatment (800C for 20, 40, and 60s).

Fig. 2 6K photoluminescence linewidth of the as-grown and RTA (700C, 800C, and 900C for 30s) MQW structures.

Fig. 3(a) Bias dependence of the spectral response for the as-grown QWIP at 80K.

Fig. 3(b) Bias dependence of the spectral response measured for the RTA QWIP at 4.5K.

Fig. 4(a) P (dashed line ) and Ga (solid line) compositions versus z(the coordinate in growth direction).

Fig. 4(b) Calculated bandgap as a function of the annealing time at 800C. Dashed curve: with both P and Ga interdiffusion. Dotted curve: with P interdiffusion only. Filled squares: 6K photoluminescence data. The second solid line is just the first dashed curve down-shifted by 20 meV to match the experiment.

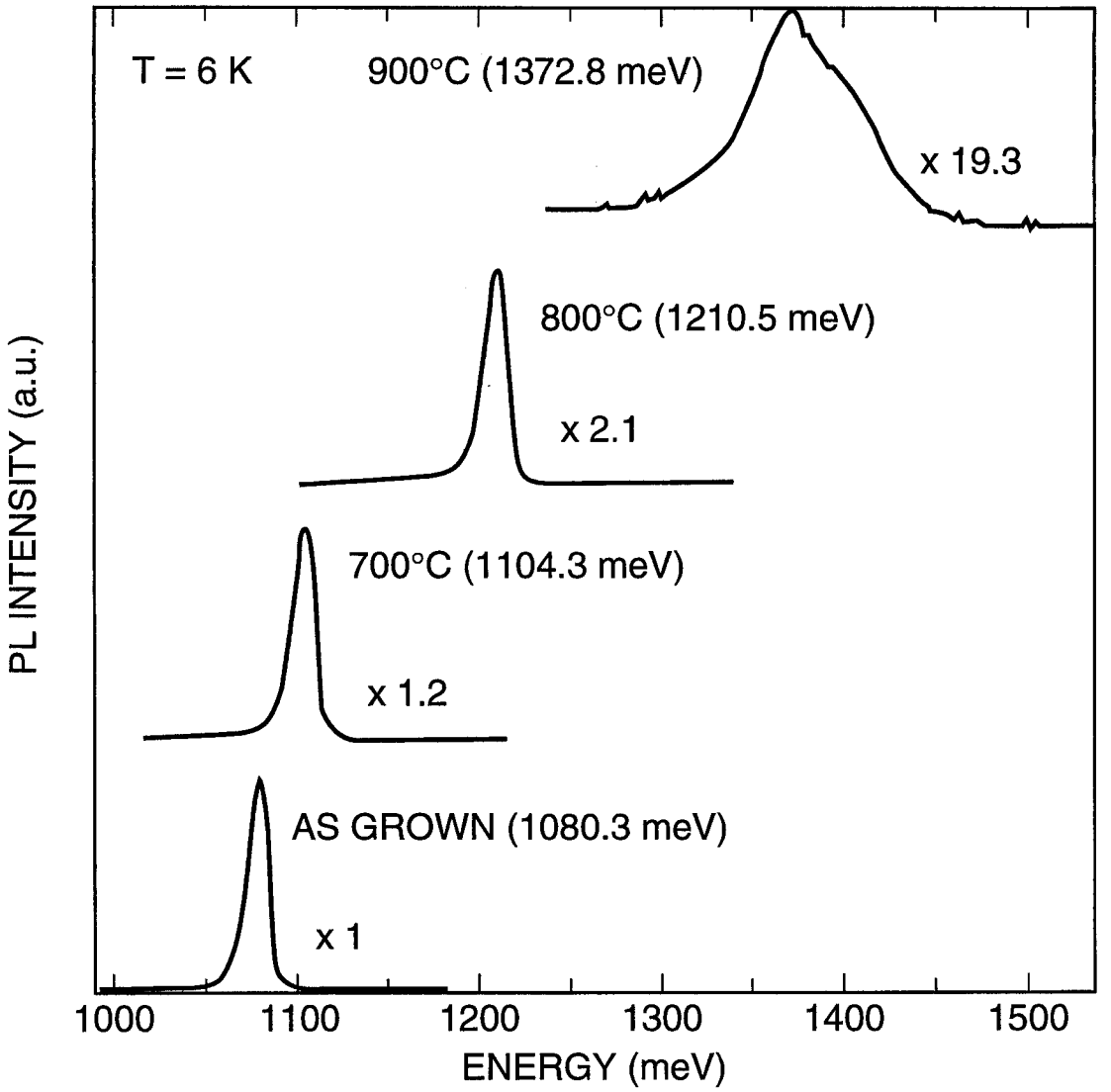


**Figure 1(a):** Photoluminescence spectra at 6K of the as-grown and RTA (700C, 800C, and 900C for 30s) MQW structures.

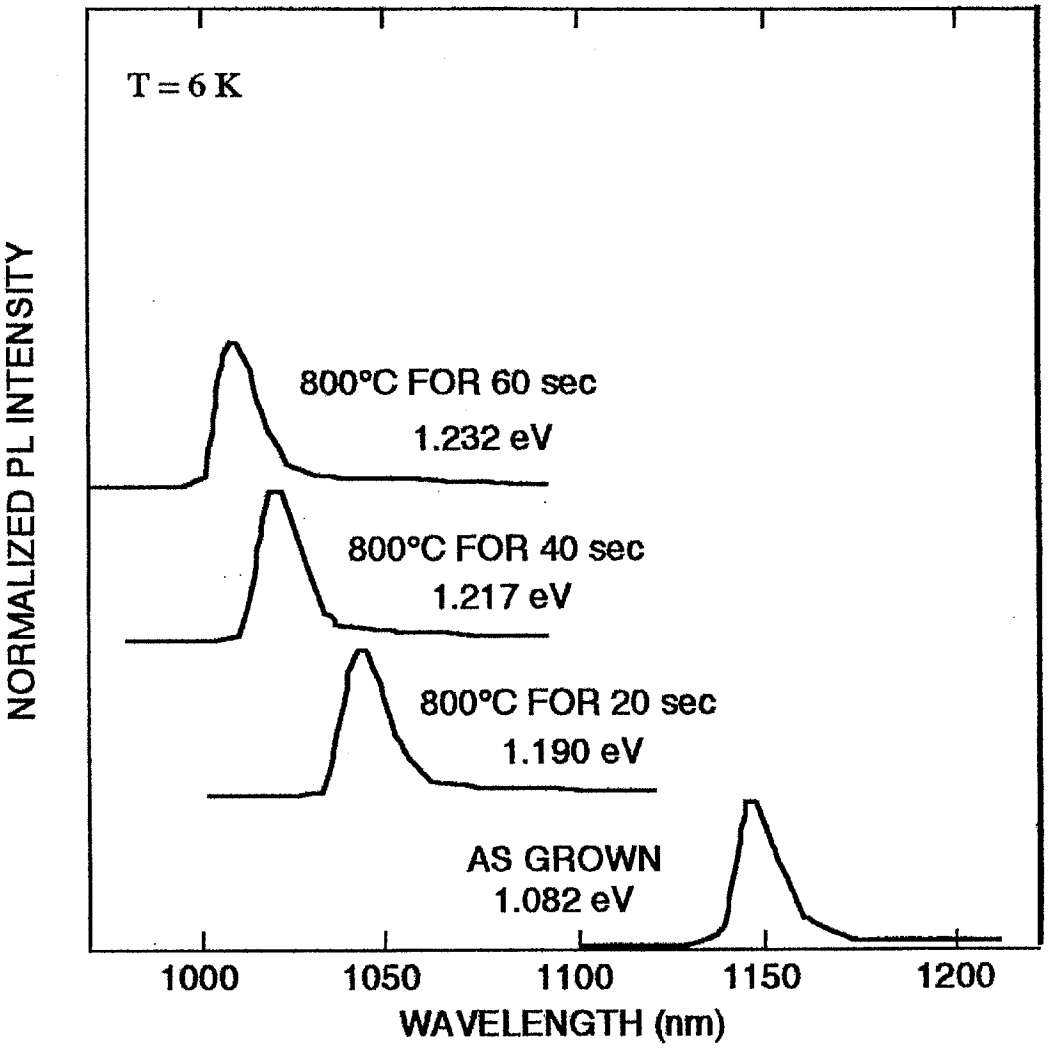


**Figure 1(b):** 6K photoluminescence spectra of the as-grown and RTA treatment (800C for 20, 40, and 60s).

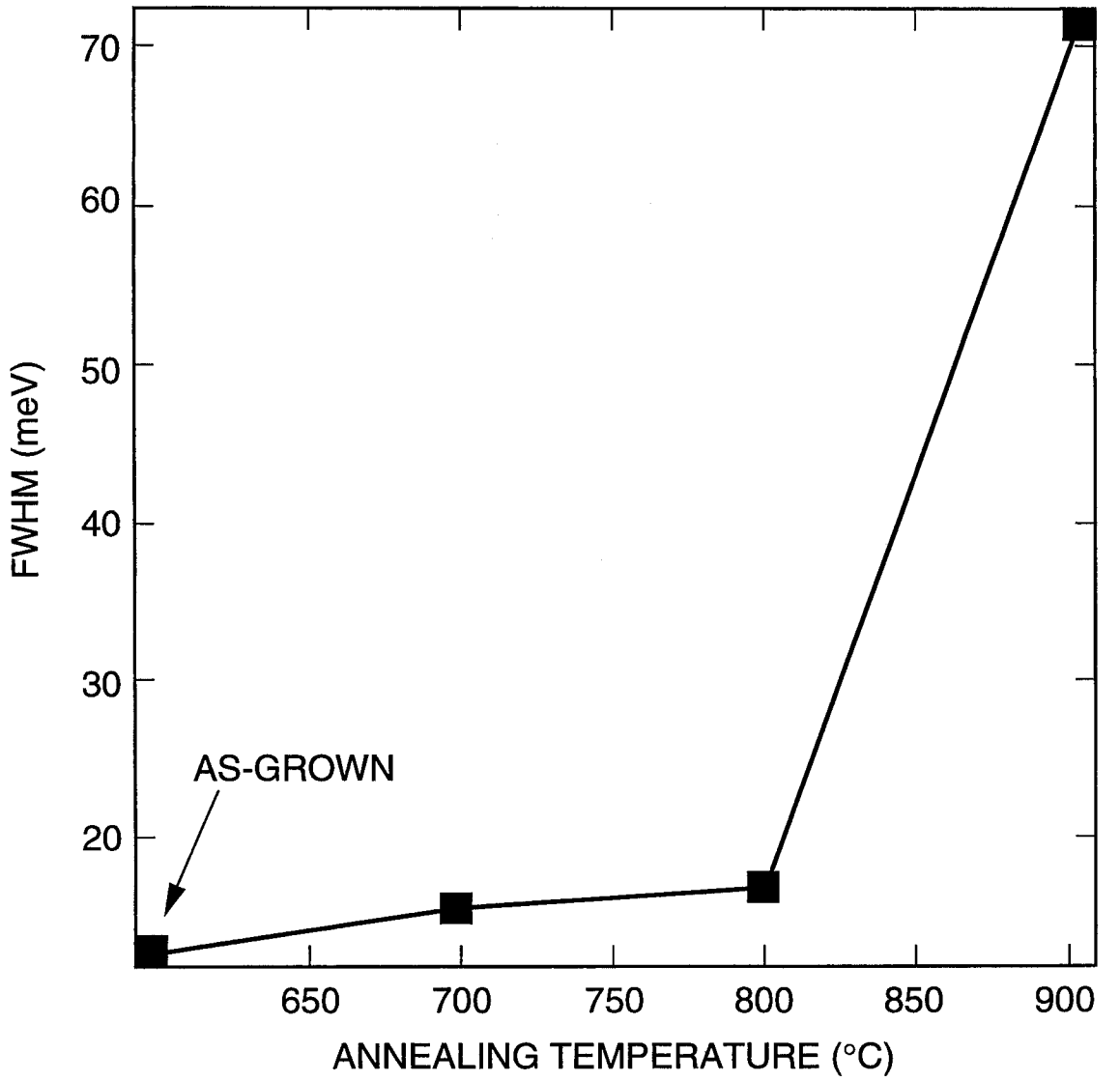


**Figure. 2:** 6K photoluminescence linewidth of the as-grown and RTA (700C, 800C, and 900C for 30s) MQW structures.

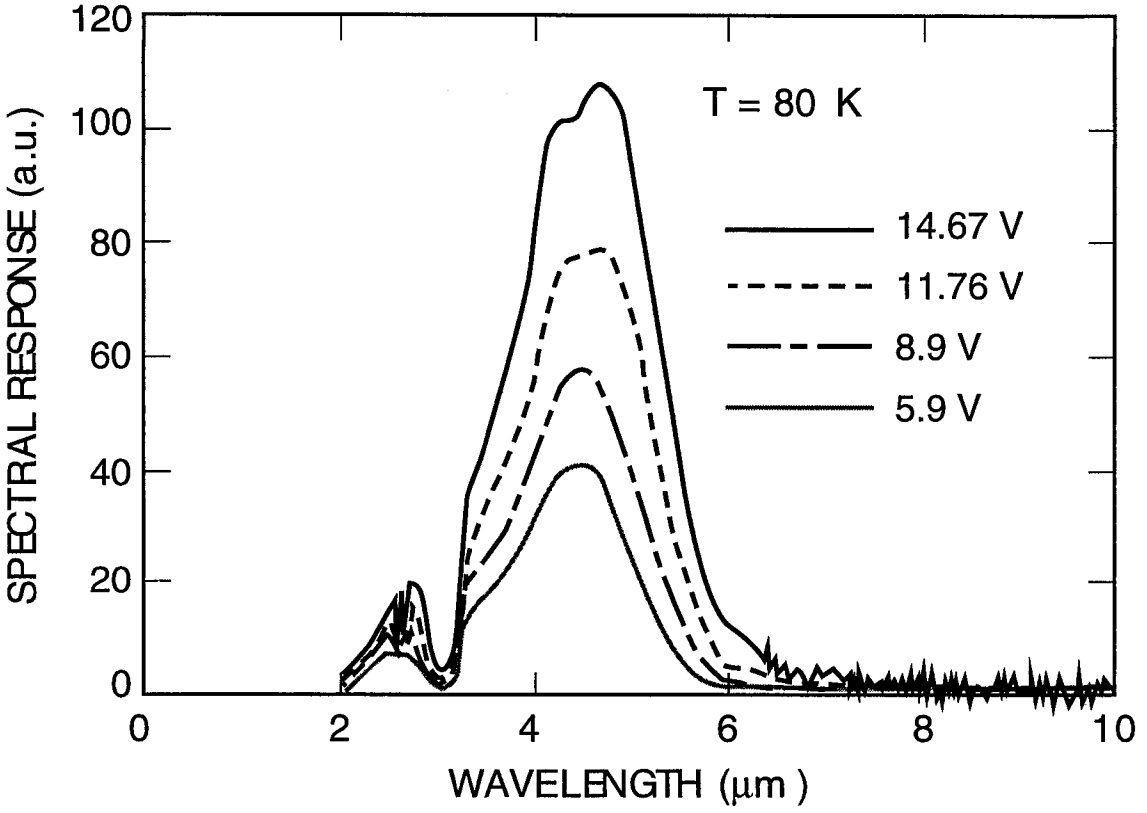


**Figure 3(a):** Bias dependence of the spectral response for the as-grown QWIP at 80K.

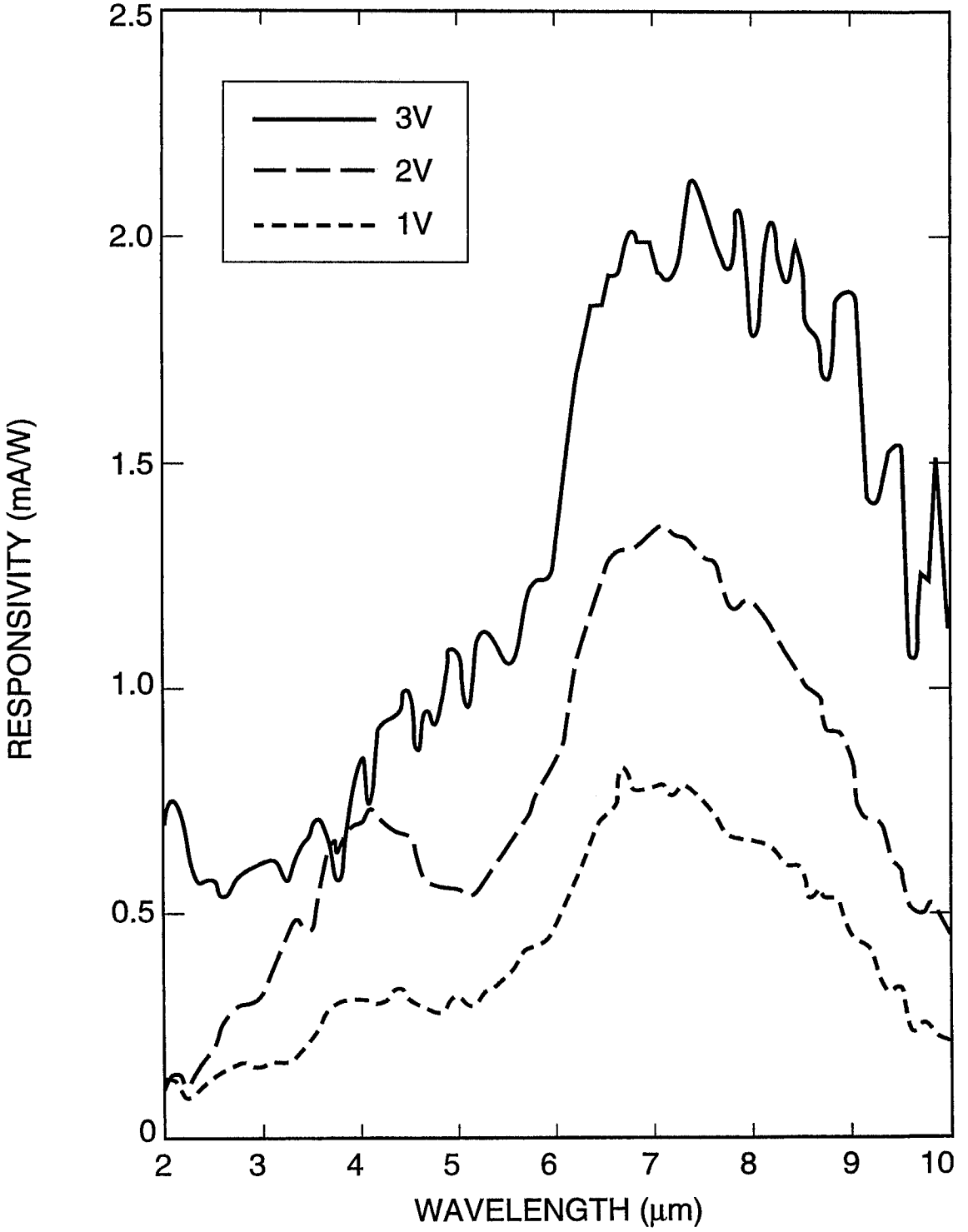


**Figure 3(b):** Bias dependence of the spectral response measured for the RTA QWIP at 4.5K.

| Material | $E_v$(eV) | $E_C$ (eV) | $\gamma_1$ | $\gamma_2$ | $\gamma_3$ | $m_c/m_0$ |
|---|---|---|---|---|---|---|
| InAs | 0.000 | 0.417 | 19.670 | 8.370 | 9.290 | 0.023 |
| InP | –0.420 | 1.002 | 6.280 | 2.080 | 2.760 | 0.077 |
| $In_{0.53}Ga_{0.74}As_1$ | 0.000 | 0.814 | 13.645 | 5.423 | 6.287 | 0.043 |
| $In_{0.53}Ga_{0.74}P$ | –0.53 | 1.578 | 5.302 | 1.563 | 2.243 | 0.077 |

**Table I. Input Parameter Used in the Present Calculation**

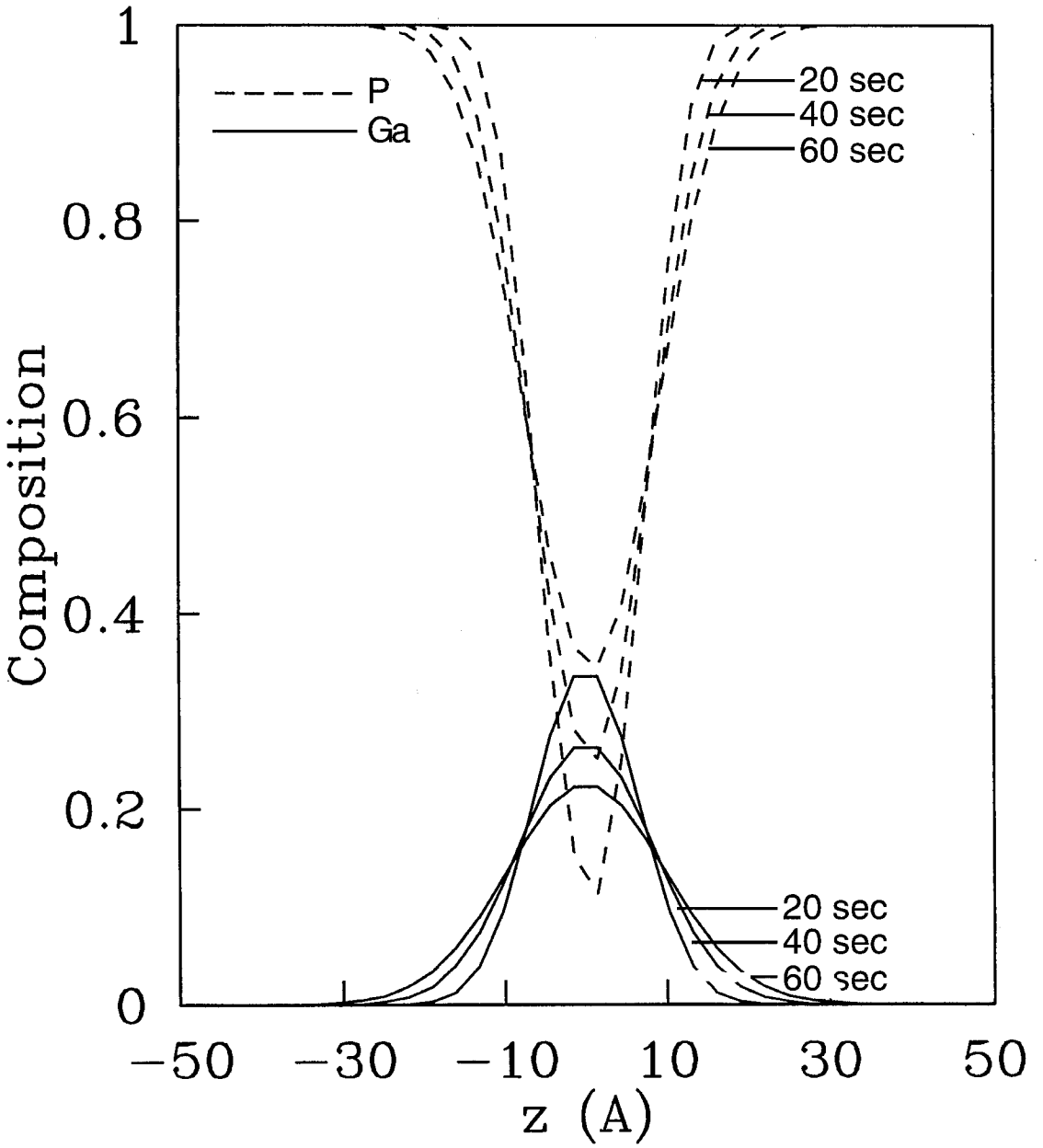


**Figure 4(a):** P (dashed line ) and Ga (solid line) compositions versus z (the coordinate in growth direction).

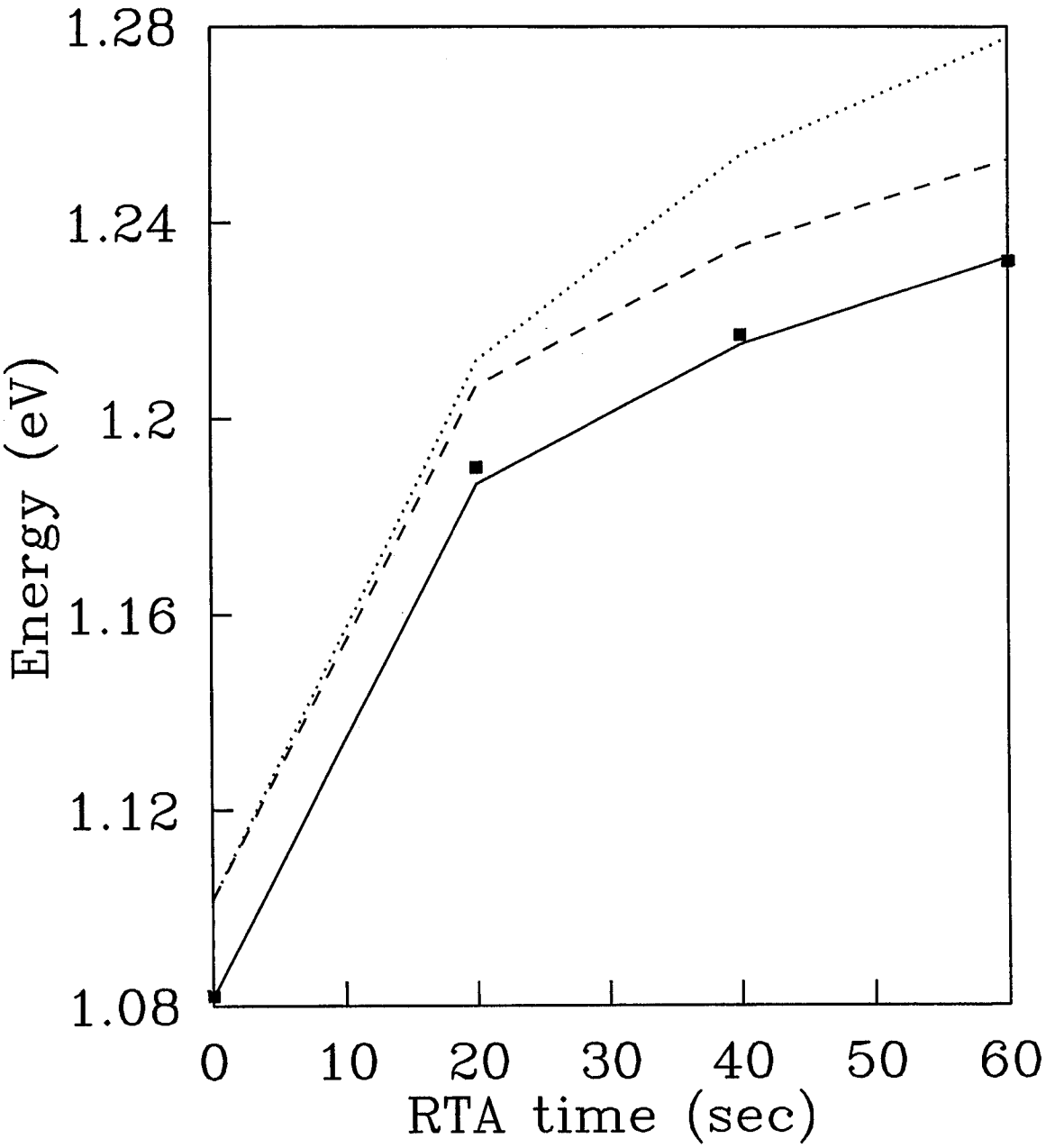


**Figure 4(b):** Calculated bandgap as a function of the annealing time at 800C. Dashed curve: with both P and Ga interdiffusion. Dotted curve: with P interdiffusion only. Filled squares: 6K photoluminescence data. The second solid line is just the first dashed curve down-shifted by 20 meV to match the experiment.